GASEOUS OXYGEN AND HYDROGEN EMBRITTLEMENTS OF A U-7.5 Nb - 2.5 Zr ALLOY

D. Lepoutre, A.M. Nominé and D. Miannay

Commissariat à l'Energie Atomique , Service Métallurgie
B.P. N° 511 - 75752 Paris Cédex 15 (France)

ABSTRACT

The occurence of gaseous oxygen and hydrogen embrittlements of a U-7.5 Nb - 2.5 Zr alloy as a function of stress intensity factor, temperature and pressure is investigated via fracture mechanics. The crack growth rate is determined. Whence only cracking occurs in oxygen and embrittlement is due to an oxidation reaction, hydriding occurs at high pressure of hydrogen and the mechanism of cracking at lower pressure is not identified.

KEYWORDS

Uranium alloys ; U-7.5 Nb - 2.5 Zr ; Oxygen embrittlement ; Hydrogen embrittlement ; Fracture mechanics ; Crack growth rate.

INTRODUCTION

Uranium alloys with high molybdenum, niobium or zirconium content can retain their high temperature stable body-centered-cubic structure at low temperature by quenching. Their mechanical resistance is high and they have much more oxidation and corrosion resistances than leaner alloys. However they are very susceptible to stress corrosion cracking and particularly in air at room temperature. A previous study on the U-10 Mo alloy (Corcos, 1979) has tried to identify the mechanisms of embrittlement in oxygen and hydrogen which are two constituents of air, the second one being released from the reaction of water vapor with the alloy, but this study was only partly successfull. So a study on the U-7.5 Nb - 2.5 Zr alloy was undertaken with the aim to corroborate the results obtained with the U-10 Mo alloy and to precise the mechanisms. The U-7.5 Nb - 2.5 Zr alloy has in fact in the quenched state a structure different from γ, the b.c.c. structure γ^o, with a parameter double of that of γ. This structure becomes tetragonal, γ^o_d, by ageing at low temperature. Moreover, the s.c.c. behavior of this alloy in air is similar to that of U-10Mo, except that the initiation stage when testing smooth specimens seems to be extremly long (Peterson, 1964).
The purpose of this paper is to present the results of the determination of the phenomenon occurence in stress, pressure and temperature and of the kinetics of crack growth using fracture mechanics. The discussion will try to identify the mechanisms of embrittlement.

ALLOY AND EXPERIMENTAL PROCEDURE

The cast U-7.5 Nb - 2.5 Zr alloy was homogenised 16 hours at 1000°C, rolled at 940°C, then water quenched. The plates were aged 1 hour at 150°C. The chemical analysis, the tetragonal parameter c/a, the hardness and the mechanical properties are given in table 1.

TABLE 1 Chemical weight analysis, tetragonal parameter c/a, hardness and mechanical properties of the alloy.

	Nb 10^{-2}	Zr 10^{-2}	O 10^{-6}	H 10^{-6}	N 10^{-6}	C 10^{-6}	Al 10^{-6}	Fe 10^{-6}
Hydrogen testing	7.5	2.3	350	16	22	85	17	61
Oxygen testing	6.7	2.1	300	17	13	75	22	67

	c/a	$H_{v(30hbar)}$	$\sigma_{Y0,2}$ MPa	σ_M MPa	A_r %	K_M MPa $\sqrt{m}$
Hydrogen testing	0.700	271	800	950	10	50
Oxygen testing	0.682	187	-	-	-	-

The tensile properties were determined at a strain rate of $2.2\ 10^{-3}\ s^{-1}$ and the toughness is the value corresponding to the load maximum in an invalid test with 4 mm thick specimens where non brittleness occurs. These values are mean values for the two plates and it is known elsewhere that toughness does not vary with temperature between - 60°C and + 60°C. The grain diameter is 70 µm.
The S.C.C. testing method has been already well documented (Corcos, 1979) and the details are not given here. Fatigue precracking is done with K_{If} Max = 10 MPa $\sqrt{m}$ in nitrogen which is shown to be inert at room temperature ($K_{ISCC} > K_Q$). Testing is done in high purity gases flowing at 0.15 MPa pressure. Partial pressures are obtained by mixing the gas with nitrogen. For oxygen, the testing temperature range is - 20°C, + 100°C, the pressure range $0.15\ 10^{-2}$, 0.15 MPa and for hydrogen, - 50°C, + 140°C and $0.15\ 10^{-2}$, 0.15 MPa.

GASEOUS OXYGEN EMBRITTLEMENT

Figure 1a shows the range of initial stress intensity factors and of temperatures where failure takes place in less than 2000 hr at 0.15 MPa(zone I), and where internal cracking at midthickness occurs as revealed by subsequent rupture under nitrogen after 2000 hr, although no cracking has occured on the face observed during testing (zone II). K_{ISCC} is taken as the lower limit. Unlike U-10 Mo where maximum susceptibility was observed at 60°C, with no cracking below 0°C, the susceptibility of U-7.5 Nb - 2.5 Zr increases with increasing temperature. As to the incubation time, figure 1b shows that it decreases with increasing temperature and is longer than the incubation time for U-10 Mo. So, while in U-10 Mo there is a critical minimum temperature and a susceptibility decreasing at high temperature, which may be due to a loss of constraint, in U-7.5 Nb - 2.5 Zr the critical minimum temperature is less than - 20°C and the susceptibility is enhanced by temperature which may be due to a phase transformation.
Propagation as observed on the surface is discontinuous with roughly three stages : after an incubation period with building of a plastic zone, cracking occurs at a constant rate and then accelerates more and more when approaching rupture. The variation of growth rate da/dt versus K_I as obtained after fitting a smooth curve to

data points is shown in figure 2 : the relative position of the curves at the same temperature may be due to scattering between specimens or to the initial value of K_I introducing a perturbation. Crack growth is thermally activated and the kinetics can roughly be fitted by the equation :

$$\frac{da}{dt} = 0.220\left[\exp\left(-\frac{5\ 10^4}{RT}\right)\right].\left(\frac{K}{50-K}\right)^2$$

with da/dt in $m.s^{-1}$ and the activation energy in $J.mole^{-1}$. 50 MPa $\sqrt{m}$ is roughly the toughness of the alloy in the investigated temperature range. The apparent activation energy is comparable to the apparent activation energy for oxidation which is 5.10^4 $J.mole^{-1}$ between 150°C and 300°C with a parabolic law under an unknown oxygen pressure (Cathcart and Peterson, 1972), $2.5\ 10^4 J.mole^{-1}$ between 22 and 100°C and $4.2\ 10^4 J.mole^{-1}$ between 100 and 200°C with a parabolic law under an air pressure of 0.087 MPa (Larson, 1971), the limiting step in the oxidation mechanism being oxygen diffusion through the oxide film governed by the potential gradient below 100°C and by concentration gradient above 100°C with an activation energy lower than the oxygen diffusion energy in pure U O_2. The oxide thickness is about 15 nm in air at 22°C after 25 hr and no oxygen is found in the alloy.
On the surface, crack propagation morphology is very similar to that in the U-10 Mo alloy (Miannay, 1977). After loading, the plastic zone builds up around the tip into two fans which join together ahead. There, a microcrack occurs and spreads towards the main crack. Then the process is repeated until K_I is near to the toughness when a large plasticity zone coarsens, in which propagation accelerates. The fracture surface shows the flat, quasi-cleavage fracture mode with the "fan-shaped" aspect in the constant rate stage (figure 3) which has been already found in the S.C.C. of the alloy in air (Magnani, 1970) and in the U-10 Mo alloy (Corcos, 1979). In the accelerating stage, the surface shows moreover some dimples, the dimples being the characteristic of the final rupture. In the specimens with internal microcracking, the S.C.C. pattern is continuous from the fatigue crack. All these observations lead us to conclude that the apparently discontinuous cracking is due to tunneling inside the specimen. Otherwise, ionic microprobe analysis of cut specimens shows that no oxygen is in the alloy near to the failure surface.
Under a pressure of $0.15\ 10^{-2}$ MPa at 20°C, K_{ISCC} is 30 MPa $\sqrt{m}$ i.e. greater than 13 MPa $\sqrt{m}$, the value under 0.15 MPa. Moreover the growth rate is equal to the growth rate under 0.15 MPa. So the critical pressure is below $0.15\ 10^{-2}$ MPa, which is in agreement with the result of Magnani (1970).
To explain this embrittlement, two types of mechanisms can be advocated. In the truly brittle aspect, oxygen adsorption or absorption can lower the binding energy or the cohesive strength ; on the other hand, oxide film can contribute to embrittlement by repeated cracking or by generating supplementary external stresses at the tip. If plasticity is taken into account, embrittlement could be due to increasing yield stress to overcome the cleavage stress. Actually, pressure is high enough to allow oxidation and not adsorption on a smooth surface. If crack geometry is taken into account, the crack tip opening is greater than $K_I^2 / E\ \sigma_Y$ = 10 µm with E = 56,000 MPa, i.e. slightly greater than the mean free path of the oxygen molecules for the pressure of $0.15\ 10^{-2}$ MPa, 5 µm. If surface roughness is taken into account, the discrepancy is lower. So, adsorption is likely at the advancing crack tip, when the gas flow regime can be changed at the lower pressure, but not at the higher pressure. As the kinetics are alike this mechanism is not sufficient to explain the embrittlement.
As to the oxidation aspect, some coherency stresses can be generated between the coherent corrosion product and the alloy. These stresses could explain the build up of plasticity at the tip at rest, if this had not yet been explained by crack tunneling. These coherency stresses have been advocated for cracking of U-Nb-Zr in oxygen at 360°C (Chirigos, 1959) with an activation energy of 10.8 $10^4 J.mole^{-1}$ equal to the activation energy of oxygen diffusion in U O_2 and for creep of unstressed, oxidised U-7.5 Nb - 2.5 Zr between 750 and 900°C (Cathcart and Liu, 1973).

The unresolved question,as first put by Chirigos, would be the fact that failure in the metal occurs at a time subsequent to maximum adherent film build-up with, moreover, the fact that the film is much thinner at lower temperature except if stresses modify the oxidation of the alloy. Likewise, the mechanism of the repeated break-down of brittle oxide film is possible, the inherent UO_2 brittleness being increased by zirconium and decreased by niobium (Armstrong,1964 ; Cathcart,1976). In earlier versions of this model, the film rupture occurs when some thickness is obtained. However a modified model can be proposed, similar to the transgranular cracking of austenitic steels in aqueous chloride solutions which exhibits the same fracture surface, where here the destructive process would be the dissolving oxidation of the active slip planes and the protective process is the passiving oxidation of the rupture faces, some critical challenging between the two processes being for cracking occurence. These ideas are presently being explored.

HYDROGEN EMBRITTLEMENT

The S.C.C. map under 0.15 MPa is shown in figure 4 : all specimens failed even under no load. At -20°C and +20°C, corrosion occurs along the fatigue crack, at the crack tip and at some inclusions, probably carbides, all over the observed surface before loading and after a few minutes after hydrogen was allowed to flow over the specimen. At -50°C, corrosion occurs later after loading, the load being applied two hours after hydrogen flow allowance. During exposure, there is no cracking but a growth of the corroded areas(figure 5) which join together up to final rupture. The process, as shown by the study of the growth rate, is thermally and mechanically activated with an apparent activation energy of $4.2\ 10^4$ J.mole^{-1}. This energy is comparable to the activation energy for hydrogen diffusion (at high temperature 800 - 1000°C) in U-7.5 Nb - 2.5 Zr:3.00 10^4J.mole^{-1} (Powell and Condon, 1973). Spalled powder of corroded specimens at ambient temperature was identified as hydrides (Zr,H)(Vaughan,1956)and(UH_3)$_\beta$, but with a lack of an intense ray in(UH_3)$_\beta$,(211)or as a b.c.c.crystal structure with a lattice parameter slightly expanded to that of the unhydrided alloy (0.727 nm versus 0.693 nm). This phase will be a metastable hydride, like in U-10 Mo where this kind of structure is observed at 140°C. This result is in agreement with the observation of Sprague (1976) that U-7.5 Nb - 2.5 Zr alloy can form hydride phases at low temperatures.

The S.C.C. map at the ambient temperature and under varying pressure is shown in figure 6 : cracking occurs to lead to failure with a crack growth rate roughly equal to the rate under oxygen or internally at a pressure of 0.15 10^{-1}MPa and there is no cracking at 0.15 10^{-2} MPa. So susceptibility is decreasing with decreasing pressure and there may be a critical pressure under which no cracking occurs. The cracking morphology on the observed surface and the rupture surface (figure 7) show the same pattern as that found under oxygen.

Complementary tests under 0.15 10^{-2} MPa with K_{Ii} = 20 MPa$\sqrt{m}$ at 100°C and 140°C show internal cracking. No hydride is revealed on the rupture surface which exhibits always the "fan-shaped" pattern. No hydride is observed in the alloy near the fracture surface of cut specimens. On the faces of the specimens a tarnished film is formed, which is radiocristallographically analysed as UO_2. So, during testing, the alloy gets the residual oxygen content of the gas which is as low as $2\ 10^{-6}$. But this residual pressure of oxygen seems not to be responsible for the embrittlement according to our preceding results about oxygen embrittlement.

Unlike U-10 Mo for which the wedging action of an hydride was emphasised in the embrittlement process, in the U-7.5 Nb - 2.5 Zr hydride occurs at higher pressure and leads to banal corrosion ; there is no hydride formation at lower pressure and the embrittling mechanism must be very similar to that occuring in oxygen environment,although hydrogen solubility is said to be high in the U-7.5 Nb - 2.5 Zr alloy and hydrogen does not affect greatly the cohesive strength of the alloy (Powell and Condon, 1976). Such a similar behavior has been already observed in the titanium alloy TA6V under hydrogen for which cracking was observed at high

stress intensity factor and hydriding at lower stress intensity factor, cracking and hydriding blunting being two competitive processes. An adsorption mechanism is to day proposed as the embrittling process. Much work is to be done to get better understanding.

ACKNOWLEDGEMENT

The authors would like to express their gratitude to the Commissariat à l'Energie Atomique which supplied facilities for this research and which allowed publication of this paper.

REFERENCES

Armstrong, W.M., and W.R. Irvine (1964). Creep of urania-base solid solutions. J. Nucl. Mater., 12, 261-270.

Cathcart, J.V., and G.F. Petersen (1972). The low temperature oxidation of U Nb and U Nb Zr alloys. J. Nucl. Mater., 43, 86-92.

Cathcart, J.V., and C.T. Liu (1973). The mechanical properties of two uranium alloys, and their role in the oxidation of the alloys. Oxidation of Metals, 6, 123-143.

Cathcart, J.V. (1976). Gaseous oxidation of uranium alloys. In J.J. Burke (Ed.), Physical metallurgy of uranium alloys, First ed. Brook Hill Publishing Company Chestnut Hill, Massachusetts, p. 775-813.

Chirigos, J.N. (1959). The role of lattice mismatch between oxide and metal in the corrosion behavior of gamma uranium alloys. In T.H. Rhodin (Ed.), Physical metallurgy of stress corrosion fracture, Vol. 4, AIME Interscience Publishers John Wiley, New-York, p. 70-78.

Corcos, J. (1979). Fragilisation de l'alliage U-10 Mo dans les milieux gazeux oxygène et hydrogène. Thesis, Paris.

Larson, D.T. (1971). Oxidation of a ternary uranium alloy. J. Vacuum Sci. Technol., 8, 80-83.

Magnani, N.J., H. Romero, and C.J. Miglionico (1970). A study of the stress corrosion cracking behavior of mulberry. Tech. Report SC RR 70 371.

Miannay, D., J. Corcos, and A.M. Nominé (1977). Gaseous oxygen and hydrogen embrittlements of a U-10 Mo alloy. In D.M.R. Taplin (Ed)., Advances in Research on the strengh and fracture of materials, Vol 2A, 4th international conference on fracture, Waterloo Canada, Pergamon Press, p. 261-267.

Peterson, C.A.W., and R.R. Vandervoort (1964). The properties of a metastable gamma uranium alloy U 7.5 Nb 2.5 Zr. Tech. Report UCRL 7869.

Powell, G.L., and J.B. Condon (1973). Mass spectrographie determination of hydrogen thermally evolved from uranium and uranium alloys. Anal. Chem., 45, 2349-2354.

Powell, G.L., and J.B. Condon (1976). Hydrogen in uranium alloys. In J.J. Burke (Ed.), Physical metallurgy of uranium alloys, First ed. Brook Hill Publishing Company, Chestnut Hill, Massachusetts, p.427-461.

Sprague, T.P. (1976). Cited in Powell, G.L., and J.B. Condon (1976). Hydrogen in uranium alloys. In J.J. Burke (Ed.). Physical metallurgy of uranium alloys, First ed., Brook Hill Publishing Company, Chestnut Hill, Massachusetts, p.427-461.

Vaughan, D.A., and J.R. Bridge (1956). J. Metals, May, 528.

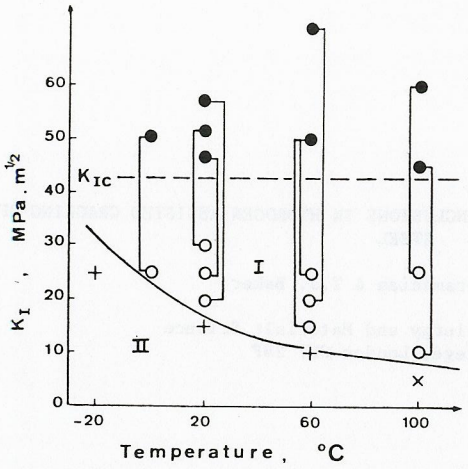

a: S.C.C. map

○ K_{Ii}, ● K_{Is} failed
+, × K_{Ii} unfailed ; + with internal propagation ; × without propagation

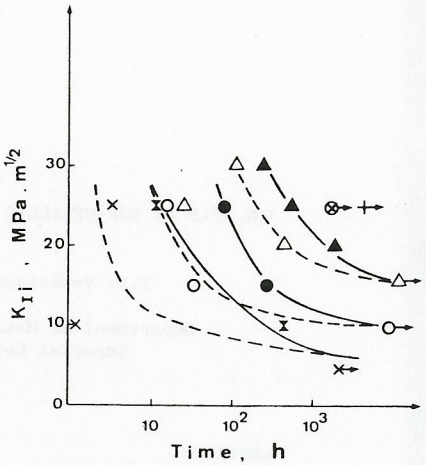

b: incubation and failure time

×, ○, △, ⊗, + incubation – – –
ⵠ, ●, ▲ failure ——
×, ⵠ 100°C ; ○, ● 60°C ; △, ▲ 20°C
⊗ 0°C ; + -20°C

Fig.1 : Tests in oxygen at 0.15 MPa

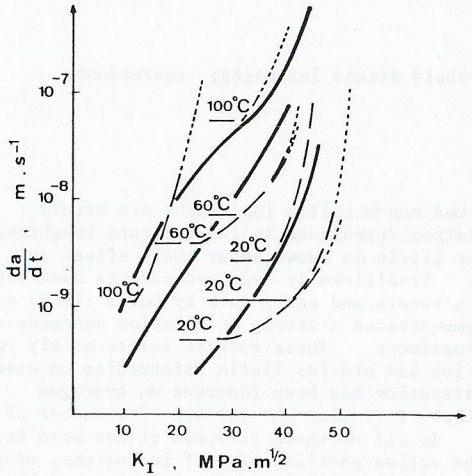

Fig. 2 : Crack growth rate in oxygen at 0.15 MPa

$\frac{da}{dt} = 0.220\left[\exp\left(-\frac{50000}{RT}\right)\right]\left(\frac{K}{50-K}\right)^2$ ——

↑ Crack propagation

Fig. 3 : Rupture surface in oxygen at 0.15 MPa

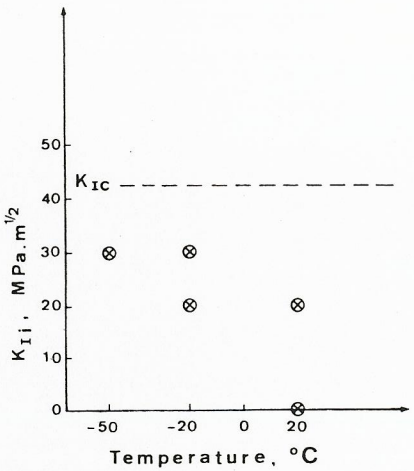

Fig. 4 : S.C.C. map in hydrogen at 0.15 MPa

⊗ corrosion

Fig. 5 : Corroded area in hydrogen at 0.15 MPa

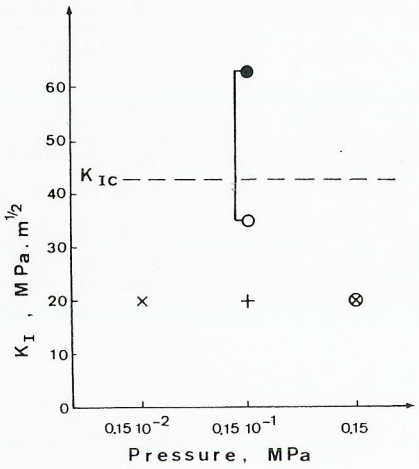

Fig. 6 : S.C.C. map in hydrogen

○ K_{Ii}, ● K_{Is} failed ;
×, + unfailed ; × without propagation ; + with internal propagation ; ⊗ corrosion

↑ Crack propagation

Fig. 7 : Rupture surface in hydrogen at 0.15 10^{-1} MPa